Hindawi Publishing Corporation
International Journal of Carbohydrate Chemistry
Volume 2012, Article ID 840591, 6 pages
doi:10.1155/2012/840591

Research Article

Preparation and Characterization of Chitosan/Zinc Oxide Nanoparticles for Imparting Antimicrobial and UV Protection to Cotton Fabric

M. M. AbdElhady

Textile Research Division, National Research Centre, Dokki, Egypt

Correspondence should be addressed to M. M. AbdElhady, marwa_abdalhady@yahoo.com

Received 27 December 2011; Revised 30 January 2012; Accepted 6 February 2012

Academic Editor: R. J. Linhardt

Synthesis of chitosan/ZnO nanoparticles was performed using different concentrations of ZnO at different temperatures. Nanoparticles of ZnO/chitosan were prepared in rod form with average length 60 nm and average width 5–15 nm. Thus, obtained nanoparticles of ZnO/chitosan were characterized using UV spectrophotometer, FTIR, TEM, X-ray, and SEM. Size and shape of chitosan/ZnO nanoparticles relied on conditions of their synthesis. Notably, chitosan/ZnO in rod form with average length of 60 nm and average width 5–15 nm could be achieved. Application of chitosan/ZnO nanoparticles to cotton fabric conferred on the latter antibacterial and UV protection properties. Cotton fabric was characterized using SEM, ultraviolet protection factor (UPF) rating, and antibacterial (gram-positive and gram-negative) characteristics. Finished cotton fabric exhibited good antibacterial properties against gram-positive and gram-negative bacteria. The UV testes indicated a significant improvement in UV protection of finished cotton fabric which is increasing by increasing the concentration of nanoparticles of ZnO/chitosan.

1. Introduction

Chitin, the second most abundant biopolymer, widely distributes in nature as the principal component of exoskeletons of crustaceans and insects as well as of cell walls of some bacteria and fungi. It is a glucose-based unbranched polysaccharide. It differs from cellulose at the C-2 carbon where an acetamido residue locates instead of a hydroxyl group. Chitosan is a partially deacetylated polymer of acetyl glucosamine obtained through alkaline deacetylation of chitin. It is a compound polymer of glucosamine and N-acetyl glucosamine. The term chitosan refers to a group of polymers varying in molecular weight upward to several million Daltons [1]. The structure of chitosan is very similar to that of cellulose; it consists of β(1-4)-linked D-glucosamine residue with the 2-hydroxyl group being substituted by an amino or acetylated amino group. The primary amine groups endow chitosan with many special properties, making it applicable in many areas and readily available for chemical reactions, for example, salt formation with acids. Chitosan is positively charged, making it able to adhere to the negatively charged surface. Chitosan is soluble in diverse acids and able to interact with polyanions to form complexes and gels. It holds antibacterial and antifungal properties. It is safe and nontoxic [2, 3]

With advent of nanotechnology, semiconductor nanoparticles have attracted much attention due to their novel optical, electrical, and mechanical properties. Among various semiconductor nanoparticles, nanosized zinc oxide (ZnO) particles are the most frequently studied because of their interest in fundamental study and also their applied aspects such as in solar energy conversion, varistors, luminescence, photocatalysis, electrostatic dissipative coating, transparent UV protection films, and chemical sensors. Previously, ZnO nanoparticles have been prepared by techniques including the sol-gel method [4, 5], precipitation [6], hydrothermal synthesis [7], and spray pyrolysis [8].

Over recent years, hybrid materials based on chitosan have been developed, including conducting polymers, metal nanoparticles, and oxide agents, due to excellent properties of individual components and outstanding synergistic effects simultaneously [9]. Currently, the research on the combination of chitosan and metal oxide has focused

on titanium dioxide, as titanium dioxide has excellent photocatalytic performance and is stable in acidic and alkaline solvents. Compared with titanium dioxide, zinc oxide has similar band-gap and antibacterial activity [9].

Sun protection creams and textiles are common choices to protect against UV radiation although UV radiation also weathers and degrades textiles. So many UV blocking agents are being developed to add or to improve the UV protection function of the textiles [10]. There are both organic and inorganic UV blockers. The organic blockers are also known as UV absorbers as they absorb the UV rays, whereas the inorganic blockers such as TiO_2 and ZnO efficiently scatter both UVA and UVB, the main cause of skin cancer. Compared with organic UV absorbers, inorganic blockers are now preferred due to their properties such as nontoxicity and chemical stability under UV radiation [10–12].

Since chitosan has tremendous ability to form metal complexes with zinc metal [13, 14] because of its amine groups and hydroxyl groups currently, chitosan-ZnO complex attracted great interests for its potential use as UV protector and medicament. This work is focused on (i) preparation and characterization of chitosan/zinc oxide nanorods complex using precipitation method and (ii) application of chitosan/ZnO nanoparticles on cotton fabric to impart antibacterial properties and UV protection.

2. Experimental

2.1. Materials. Mill-bleached 100% cotton fabric was kindly supplied by Misr Company for spinning and weaving Mehalla El Kobra, Egypt. Chitosan is poly [β-2-amino-2-deoxy-(1-4)-D glucopyranose] with a molecular weight of 60, 000 Da, and a deacetylation degree of 85% was supplied by Fluka. Zinc oxide (ZnO), sodium hydroxide (NaOH), and acetic acid were of laboratory grade chemicals.

2.2. Preparation of Chitosan/Zinc Oxide Nanoparticles. The accurate weight of ZnO powder (0.1–1 gm) was dissolved in 100 mL of 1% acetic acid where it changed to zinc cations. To this solution 1 gm of chitosan was added. The mixture was sonicated for 30 min. After magnetic stirring, 1 M NaOH drop by drop was added until the solution attained pH 10. The solution was heated in water bath at (40–80°C) for about 3 hr. It was then filtered and washed with distilled water several times then dried in an oven at 50°C for 1 hr.

2.3. Application Chitosan/Zinc Oxide Nanoparticles to Cotton Fabric. 0.5–4 wt % Chitosan/ZnO nanoparticles powder was suspended in water and was sonicated for 10 min. In these suspensions bleached cotton fabric samples were padded in two dip and nip and then squeezed to a wet pick-up of 100%. The samples were then dried at 100°C for 10 min and cured at 170°C for 5 min. The so treated cotton fabrics were washed with distilled water and finally dried at ambient conditions.

2.4. Characterization

2.4.1. UV-Vis Spectrum. UV-vis spectrum was recorded on Perkin Elmer Lambda 3B UV-vis spectrometer. Ultraviolet protection factor (UPF) was measured using UV Shimadzu 3101 PC spectrophotometer.

2.4.2. FTIR Spectroscopy. FTIR spectroscopy was measured using FT-IR, model: Nexus 670 (Nicollet-Madison-WI-USA). The samples were mixed uniformly with potassium bromide at 1 : 5 (sample : KBr) ratio, respectively. The KBr discs were prepared by compressing the powders (mixture of sample and KBr) at pressure of 5 tons for 5 min in a hydraulic press. The discs were scanned in the range of 400–4000 cm^{-1} to obtain FT-IR spectra.

2.4.3. Scanning Electron Microscope (SEM). Fabric samples under investigation were examined by a JEOL-840X scanning electron microscope, from Japan, magnification range 35–10,000, resolution 200 Å, acceleration voltage 19 kV. All the samples were coated with gold before SEM testing.

2.4.4. Transmission Electron Microscope (TEM). Transmission electron microscope (TEM) observation was performed on a JEOL JEM-1230 electron microscope at accelerating voltage of 120 kV. Specimens for TEM measurements were prepared by depositing a drop of colloid solution on a 400 mesh copper grid coated by an amorphous carbon film and evaporating the solvent in air at room temperature.

2.4.5. X-Ray Diffraction (XRD). XRD patterns recorded on a Philips PW 3050/10 model. The samples were recorded on a Philips X-Pert MMP diffractometer. The diffractometer was controlled and operated by a PC computer with the programs P Rofit and used a MoK (source with wavelength 0.70930 Å, operating with Mo-tube radiation at 50 kV and 40 mA.

2.4.6. Antibacterial Activity. Antibacterial activity towards *Staphylococcus aureus* (*S. aureus*, gram-positive bacteria) and *Escherichia coli* (*E. coli*, gram-negative bacteria) was evaluated using Agar Plate Method (AATCC Test Method 147-1988).

3. Results and Discussion

3.1. Preparation of Chitosan/ZnO Nanoparticles (Effect of Process Parameters). The prepared Chitosan/ZnO nanoparticles at 40–80°C in powder form were suspended in water and sonicated for 10 min then characterized by UV-vis absorbance spectra.

3.1.1. Effect of Concentration of Zinc Oxide. Figure 1 shows UV-vis absorbance spectra of chitosan and prepared chitosan/ZnO nanoparticles at 60°C. Obviously, (Figure 1, curve a), chitosan exhibits characteristic peak at 226 nm. After incorporation of different concentrations of ZnO in chitosan, this peak undergoes a characteristic peak at range 360–348 nm is which observed.

In detail, at a concentration of 0.1% ZnO (Figure 1, curve b), there is an absorption peak observed at 360 nm,

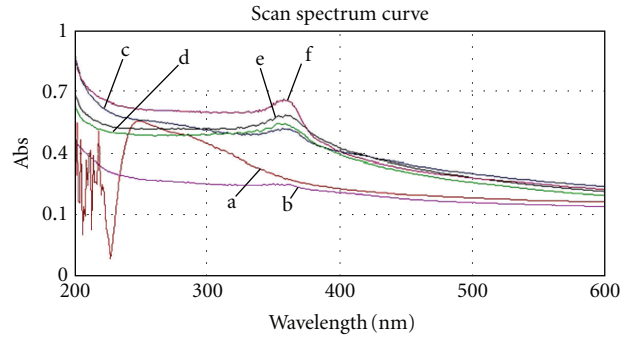

FIGURE 1: UV-vis absorbance spectra of chitosan and chitosan/ZnO nanoparticles at different concentrations. (a) chitosan, (b) chitosan/ZnO (0.1%), (c) chitosan/ZnO (0.25%), (d) chitosan/ZnO (0.5%), (e) chitosan/ZnO (0.75%) and (f) chitosan/ZnO (1%).

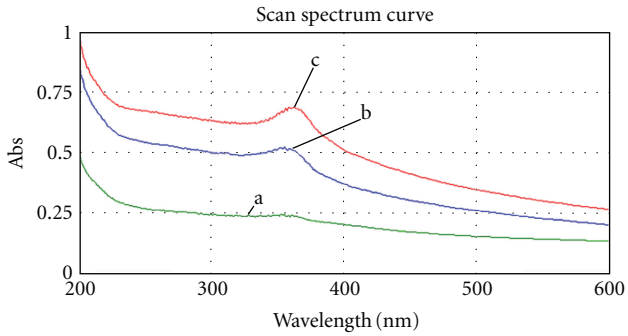

FIGURE 2: UV-vis absorbance spectra of chitosan and chitosan/ZnO (0.75%) nanoparticles at different temperatures (a) at 40°C, (b) at 60°C, and (c) at 80°C.

indicating the formation of nanoparticles of chitosan/ZnO in larger size. By increasing the concentration of ZnO to 0.25, 0.5, and 0.75% (Figure 1, curves c, d, and e), the absorption peaks are shifted to 356, 350, and 348 nm, respectively. Increasing the concentration of ZnO further to 1% (Figure 1, curve f), the absorption peak changes to about 350 nm. This could be attributed to formation of smaller nanoparticles of chitosan/ZnO complex. So that higher concentrations of ZnO are recommended.

3.1.2. Effect of Temperature. Figure 2 shows UV-vis spectra of different chitosan/ZnO nanoparticles samples prepared at 0.75%wt of ZnO and different temperatures. It is seen that, at temperature 40°C (Figure 2, spectrum a), the absorption peak is observed at 356 nm. Increasing the preparation temperature to 60°C and 80°C results in shifting towards lower absorption bands of 348 and 353 nm (Figure 2, spectra b and c). This could be attributed to complete conversion of chitosan-Zn $(OH)_2$ complexes to ZnO nanoparticles under the influence of higher temperature.

Based on the above results, it is clear that all the concentrations of ZnO used in the synthesis of chitosan/ZnO produce complexes which assume nanocrystalline form, in contrast with the macrocrystalline form with an absorption band at 372 nm when ZnO alone was used [9].

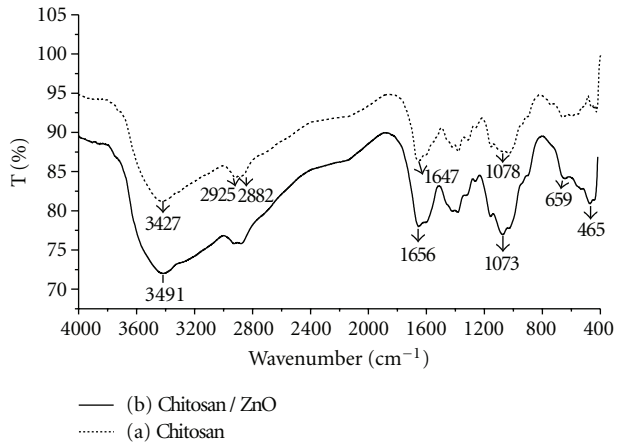

FIGURE 3: FTIR of chitosan (a) and chitosan/ZnO nanaoparticles (b).

The optimum concentration of ZnO for formation of chitosan/ZnO nanoparticles is 0.75%, and the optimum temperature is 60°C; under this condition an absorption peak at 348 nm is and shifted by 22 nm than macrocrystalline ZnO. This indicates that ZnO within chitosan complex is in the nanoscale and in full agreement with IR and X-ray analysis as will be shown latter.

3.2. Mechanism of Formation of Chitosan/ZnO Nanoparticles. When chitosan and zinc oxide are dissolved in diluted acetic acid; thereby; adjusting the acidity of solution, Zn^{2+} ions were formed. At pH = (6 to 9) the unstable compound $Zn[(OH)]_2$ was formed, according to the following equation:

$$Zn^{2+} + 2OH \rightleftharpoons Zn(OH)_2 \quad (1)$$

Since chitosan NH_2 and OH groups can form co-ordination bond with metal ions [15], by increasing pH of the solution to pH = 10 dropwise addition of NaOH, the stable complex of chitosan/ZnO nanoparticles is formed.

3.3. IR Analysis. (Figure 3, curves a and b) depicts the FTIR of chitosan and chitosan/ZnO nanaoparticles. For chitosan (Figure 3(a)) shows absorption peak at 3427 cm^{-1}. This attributed to the combined peaks of the NH_2 and OH group stretching vibration [16]. Compared with chitosan, (curve 3-b), the broader and stronger peak moved noticeably to lower wave number at 3419 cm^{-1} which indicated the strong interaction between these groups and ZnO [17]. The absorption peaks at 2925, 2882 cm^{-1} are attributed to asymmetric stretching of CH_3 and CH_2 of chitosan polymer [16]. While the absorption peaks at 1647 and 1078 cm^{-1} are ascribed to bending vibration of $-NH_2$ group and C–O stretching group, compared with chitosan, there are new absorption peaks at 659 cm^{-1} and 465 cm^{-1} which are due to the attachment of amide group and stretching mode of ZnO [18]. In addition to these results, the characteristic peaks of (Figure 3(b)) are shifted to lower wavenumber, the wide peak at 3427 cm^{-1}, corresponding to the stretching vibration of hydroxyl, amino and amide groups, moved noticeably

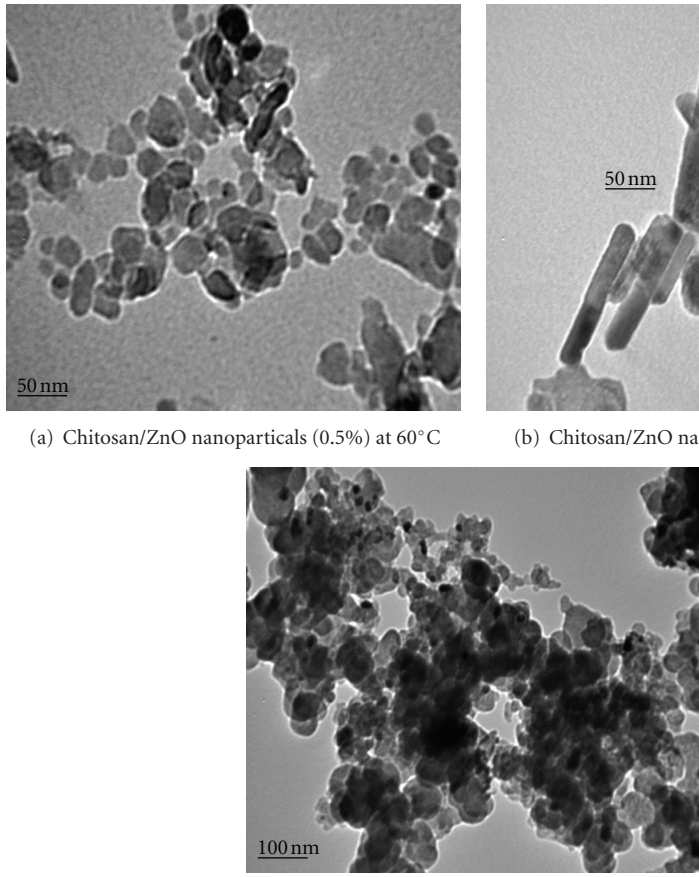

(a) Chitosan/ZnO nanoparticals (0.5%) at 60°C (b) Chitosan/ZnO nanoparticals (0.75%) 60°C

(c) Chitosan/ZnO nanoparticals (0.75%) 80°C

Figure 4: TEM photographs of chitosan/ZnO nanoparticles.

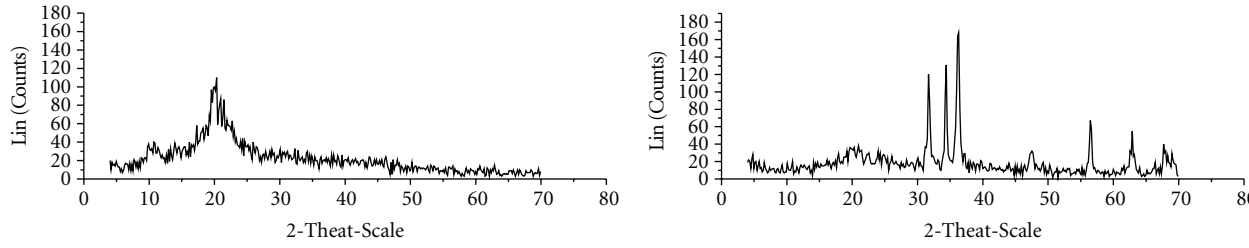

(a) (b)

Figure 5: X-ray diffraction patterns of chitosan (a) and chitosan/ZnO nanoparticles (b).

to lower wavenumbers 3419 cm^{-1}, and became broader and stronger, which indicated the strong interaction between these groups and ZnO, compared with Figure 3(a), a point which could be explained in terms of strong attachment of ZnO to the amide groups of chitosan molecules.

3.4. TEM Analysis. Figure 4 represents TEM photograph of chitosan/ZnO nanoparticles. It is evident that at concentration 0.5%, nanospheres ZnO are formed with average sizes 10–20 nm. While increasing the concentration of ZnO up to 0.75%, the average length of ZnO nanorods increases to 60 nm keeping the average width at 5–15 nm. This could be interpreted in terms of lower concentration of ZnO (0.5% at 60°C) which leads to incomplete growth of nanoparticles of chitosan/ZnO complex. On the other hand, ZnO concentrations as high as 0.75% give complete growth of nanorods. It is also evident that increasing the temperature from 60°C to 80°C is accompanied by breakingdown of nanorods to nanospheres (Figure 4(c)) with higher agglomeration of smaller size nanoparticles having 5–10 nm.

3.5. X-Ray Analysis. Figure 5 shows the X-ray diffraction patterns of chitosan and chitosan/ZnO nanoparticles. The typical peaks of chitosan (Figure 5(a)) appeared at 10.67° and 19.99° [9], while these peaks become weak in the XRD pattern of chitosan/ZnO nanoparticals (Figure 5(b)). Other

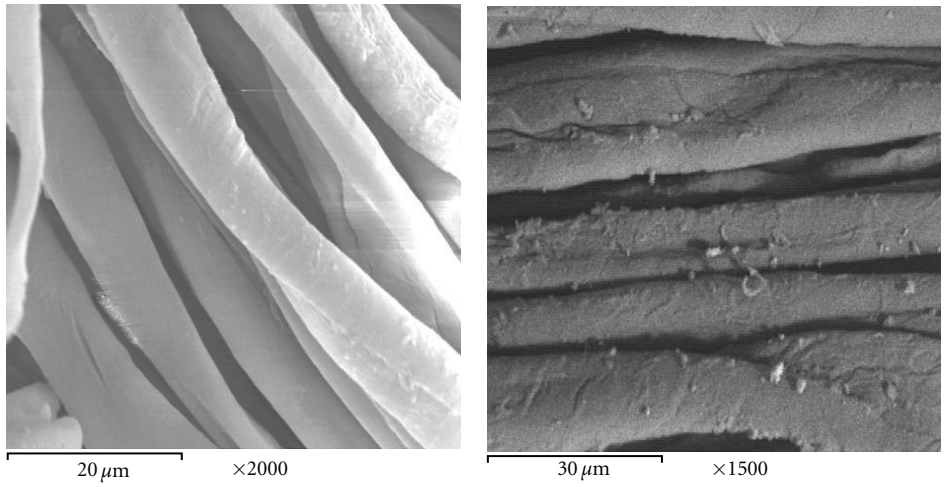

(a) Untreated cotton fabric

(b) Cotton fabric treated with chitosan/zinc oxide nanoparticles

Figure 6: SEM of cotton fabric treated with chitosan/ZnO nanoparticles.

Table 1: The antibacterial activity and UPF rating of bleached cotton fabric treated by chitosan/ZnO nanoparticles.

Concentration of chitosan/ZnO nanoparticles (%)	Inhibition zone (mm)		UPF rating
	S. aureus	*E. coli*	
0.0[a]	—	—	1.5
0.5	5	7	3.5
1	9	10	4.8
2	11	12	6.0
4	11	13	8.3

[a]Represents the untreated bleached cotton fabric.
Condition used: cotton fabric treated by chitosan/ZnO nanoparticles (0.75%) at pickup 100%, dried at 100°C for 10 min, and then cured at 170°C for 5 min.

diffraction peaks in Figure 5(b) are sharper and stronger at 31.7°, 34.36°, 36.2°, 56.59°, 62.7°, and 67.90° and were assigned to the (1 0 0), (0 0 2), (1 0 1), (1 1 0), (1 0 3), and (1 1 2) planes of hexagonal zinc oxide can be indexed to the wurtzite ZnO with high crystallinity. All the diffraction peaks are in good agreement with those of hexagonal wurtzite structure of ZnO (JCPDS card 36-1451) [16]. This, indeed, revealed that it is successful formation of nanosized chitosan/ZnO complex [18].

3.6. Scan Electron Microscope. The surface characteristics of untreated and chitosan/ZnO nanoparticals treated cotton fabric were examined by scanning electron microscopy, and the images obtained are shown in Figure 6. In Figure 6(a), the untreated cotton fabric seems to be a smooth fibers. While with cotton fabric treated with chitosan/ZnO nanoparticles Figure 6(b), nanoparticles are dispersed on the surface of the fiber.

3.7. Antibacterial Activity. Different cotton swatches were treated with different concentrations of chitosan/ZnO nanoparticles. These swatches were monitored for antibacterial activities. Results obtained are set out in Table 1. It is seen that the circular inhibition zone increases with increasing the concentrations of chitosan/ZnO nanoparticles in the range studied. It is also observed (Table 1) that the inhibition zone for *E. coli* is greater than the inhibition zone for *S. aureus*. This could be associated with differences in cell wall structure. At any event, however, the antibacterial activity could be attributed to the antibacterial effect of chitosan [19] and photocatalysis of ZnO.

Photocatalysis mechanism was as follows: when ZnO nanoparticles ($Eg = 3.37\,\text{eV}$) were under light irradiation, the electron transition from the valence band to the conduction band resulted in the electron-hole pair in which electron (e^-) was reductive, and hole (h^+) was oxidative. The hole (h^+) reacted with OH^- on the surface of ZnO nanoparticles, generating hydroxyl radicals (OH^-), superoxide anion ($O_2{}^-$), and perhydroxyl radicals ($HO_2{}^-$). These highly active free radicals and actual lethal agent hydrogen peroxide (H_2O_2), produced from OH^- and $O_2{}^-$, could damage the cells of bacteria, leading to decomposition, complete destruction of its internal structure, eventually, to achieve germicidal and antibacterial effects [20].

3.8. UV Protection. Table 1 shows also UV protection of bleached cotton fabric treated by chitosan/ZnO nanoparticles. It is clearly seen from that ultraviolet protection

factor (UPF) of the treated samples is higher than that of untreated cotton fabric. Also UPF rating increases by increasing the concentration of chitosan/ZnO nanoparticles from 0.5% to 4%. This reflects the capacity of UV absorption of ZnO/nanoparticles on the surface of the cotton fabric [21].

4. Conclusion

Synthesis and characterization of chitosan/ZnO nanaoparticles were investigated. Chitosan/ZnO nanoparticles were characterized using UV-vis spectrophotometer at different concentrations of ZnO and different temperature. The optimum concentration of ZnO for formation of nanoparticles is 0.75%, and the optimum temperature is 60°C. The obtained nanoparticles were investigated using FTIR, TEM, and X-ray analysis. Based on TEM results, it is shown nanoparticles in rod form with average length 60 nm and average width 5–15. Coating of cotton fabric by thus obtained chitosan/ZnO nanoparticles enhances the UV absorbing activity of treated fabric. Also the treated fabric has significant improvement at antibacterial properties. From the above results, this innovation is important because it may allow its practical use for industrial applications.

References

[1] S. Sevda and S. J. McClure, "Potential applications of chitosan in veterinary medicine," *Advanced Drug Delivery Reviews*, vol. 56, no. 10, pp. 1467–1480, 2004.

[2] S. A. Agnihotri, N. N. Mallikarjuna, and T. M. Aminabhavi, "Recent advances on chitosan-based micro- and nanoparticles in drug delivery," *Journal of Controlled Release*, vol. 100, no. 1, pp. 5–28, 2004.

[3] S. K. Kim and N. Rajapakse, "Enzymatic production and biological activities of chitosan oligosaccharides (COS): a review," *Carbohydrate Polymers*, vol. 62, no. 4, pp. 357–368, 2005.

[4] N. B. Hubbard, M. L. Culpepper, and L. L. Howell, "Actuators for micropositioners and nanopositioners," *Applied Mechanics Reviews*, vol. 59, no. 1–6, pp. 324–334, 2006.

[5] H. J. Lee, S. Y. Yeo, and S. H. Jeong, "Antibacterial effect of nanosized silver colloidal solution on textile fabrics," *Journal of Materials Science*, vol. 38, no. 10, pp. 2199–2204, 2003.

[6] L. Wang and M. Muhammed, "Synthesis of zinc oxide nanoparticles with controlled morphology," *Journal of Materials Chemistry*, vol. 9, no. 11, pp. 2871–2878, 1999.

[7] H. Y. Xu, H. Wang, Y. C. Zhang et al., "Hydrothermal synthesis of zinc oxide powders with controllable morphology," *Ceramics International*, vol. 30, no. 1, pp. 93–97, 2004.

[8] T. Tani, L. Mdler, and S. E. Pratsinis, "Homogeneous ZnO nanoparticles by flame spray pyrolysis," *Journal of Nanoparticle Research*, vol. 4, no. 4, pp. 337–343, 2002.

[9] L. H. Li, J. C. Deng, H. R. Deng, Z. L. Liu, and L. Xin, "Synthesis and characterization of chitosan/ZnO nanoparticle composite membranes," *Carbohydrate Research*, vol. 345, no. 8, pp. 994–998, 2010.

[10] G. Reinert, F. Fuso, R. Hilfiker, and E. Schmidt, "UV-protecting properties of textile fabrics and their improvement," *Textile Chemist and Colorist*, vol. 29, no. 12, pp. 36–43, 1997.

[11] H. Yang, S. Zhu, and N. Pan, "Studying the mechanisms of titanium dioxide as ultraviolet-blocking additive for films and fabrics by an improved scheme," *Journal of Applied Polymer Science*, vol. 92, no. 5, pp. 3201–3210, 2004.

[12] T. Ohno, K. Sarukawa, K. Tokieda, and M. Matsumura, "Morphology of a TiO_2 photocatalyst (Degussa, P-25) consisting of anatase and rutile crystalline phases," *Journal of Catalysis*, vol. 203, no. 1, pp. 82–86, 2001.

[13] R. A. A. Muzzarelli and L. Sipos, "Chitosan for the collection from seawater of naturally occurring zinc, cadmium, lead and copper," *Talanta*, vol. 18, no. 9, pp. 853–858, 1971.

[14] R. A. A. Muzzarelli and O. Tubertini, "Chitin and chitosan as chromatographic supports and adsorbents for collection of metal ions from organic and aqueous solutions and sea-water," *Talanta*, vol. 16, no. 12, pp. 1571–1577, 1969.

[15] A. Higazy, M. Hashem, A. ElShafei, N. Shaker, and M. M. Abdel Hady, "Development of antimicrobial jute packaging using chitosan and chitosan-metal complex," *Carbohydrate Polymers*, vol. 79, no. 4, pp. 867–874, 2010.

[16] M. Guo, P. Diao, and S. Cai, "Hydrothermal growth of well-aligned ZnO nanorod arrays: dependence of morphology and alignment ordering upon preparing conditions," *Journal of Solid State Chemistry*, vol. 178, no. 6, pp. 1864–1873, 2005.

[17] R. Salehi, M. Arami, N. M. Mahmoodi, H. Bahrami, and S. Khorramfar, "Novel biocompatible composite (Chitosan-zinc oxide nanoparticle): preparation, characterization and dye adsorption properties," *Colloids and Surfaces B*, vol. 80, no. 1, pp. 86–93, 2010.

[18] P. Bhadra, M. K. Mitra, G. C. Das, R. Dey, and S. Mukherjee, "Interaction of chitosan capped ZnO nanorods with *Escherichia coli*," *Materials Science and Engineering C*, vol. 31, no. 5, pp. 929–937, 2011.

[19] I. M. Helander, E.-L. Nurmiaho-Lassila, R. Ahvenainen, J. Rhoades, and S. Roller, "Chitosan disrupts the barrier properties of the outer membrane of Gram-negative bacteria," *International Journal of Food Microbiology*, vol. 71, no. 2-3, pp. 235–244, 2001.

[20] B. Halliwell and J. M. C. Gutteridge, "Oxygen toxicity, oxygen radicals, transition metals and disease," *Biochemical Journal*, vol. 219, no. 1, pp. 1–14, 1984.

[21] S. Kathirvelu, D. Souzaa, and B. Dhurai, "UV protection finishing of textiles using ZnO nanoparticals," *Indian Journal of Fiber and Textile Research*, vol. 34, no. 3, pp. 267–273, 2009.